Iranian Journal of Catalysis 9(4), 2019, 305-320

IRANIAN JOURNAL OF CATALYSIS

Synthesis and application of Ti-incorporated mesoporous silicate in deep oxidesulfurization of DBT from liquid fuel

Masomeh Ezati, Shohreh Fatemi*, Maede Salmasi

School of Chemical Engineering, College of Engineering, University of Tehran, P.O. Box: 11365-4563, Tehran, Iran.

Received 1 October 2018; received in revised form 30 May 2019; accepted 24 June 2019

ABSTRACT

In-situ synthesis of Ti-incorporated MCM-41 nano catalyst was carried out by the hydrothermal method to prepare a mesoporous catalyst for the oxidative desulfurization reaction (ODS). Oxidative reaction of dibenzothiophene (DBT) as a heavy sulfur compound was evaluated in a solution of n-decane as a model of liquid fuel. The synthesized catalysts were characterized by XRD, FESEM, EDX, TEM, FTIR and BET analysis and the most crystalized and purified catalyst on the base of XRD analysis was obtained at the synthesis temperature of 383 K, TIPT/TEOS=0.01, NaOH/TEOS=0.3 and TEOS/CTAB=0.2. The ODS reaction was investigated in a batch reactor in the presence of H_2O_2 as oxidant and the effect of operating conditions such as reaction temperature and molar ratio of oxidant/DBT were studied by the experimental design and the optimal operating conditions were predicted on the base of maximum DBT conversion. Removal of the produced sulfones was performed by acetonitrile as a polar solvent with the equal volume ratio of acetonitrile to model fuel. By simultaneous reaction and extraction, the DBT removal was achieved up to 99.5% during 20 min reaction. The recyclability of the prepared catalyst was studied by treatment with methanol and drying at 373 K for 4 hours. It was revealed that after two stages of reaction-regeneration, the conversion of DBT was reduced from 99.5 to 88%.

Keywords: *Oxidative desulfurization (ODS), Hydrothermal synthesis, Mesoporous catalyst, Titanosilicate, DBT conversion.*

1. Introduction

Aromatic sulfur-containing compounds and their derivatives are harmful impurities in liquid hydrocarbon fuels and they cause serious challenge for the environment. In recent years, much attention has been paid to reduce the amount of sulfur compounds present in hydrocarbon fuels [1]. Although the HDS process is the most common process of fuels desulfurization, it is very expensive in terms of operating cost and energy consumption. Also, it is difficult for refractory sulfur compounds to be treated by this process [2, 3]. Thus, a large number of non-HDS processes, such as extraction [4], adsorption [5], bio-process [6] and oxidative desulfurization [7] have been explored. Among these methods, the catalytic oxidative desulfurization (ODS) is regarded as the most promising and economical process. The ODS process, in mild conditions, atmospheric pressure and temperature range of 323-328 K, with lower cost and power consumption is a proper alternative to HDS process [3].

*Corresponding author.
E-mail address: shfatemi@ut.ac.ir (S. Fatemi)

This process involves two steps: oxidation of DBT to sulfoxides and sulfones by oxidant, and then removal of the ODS products by extraction [8].

Several oxidants have been proposed for ODS, such as hydrogen peroxide [9], tetra butyl hydroperoxide (TBHP) [8], per-acids and ozone [10]. H_2O_2 is commonly used as an oxidizing reagent due to its affordable cost, environmental compatibility, and commercial availability [5, 11]. Catalysts are responsible for activating the oxidants so they are essential in the ODS process. Different catalytic systems have been reported for these processes which include a homogenous or heterogeneous catalyst. The main problem of ODS process is the limitation of two-phase interface (fuel and oxidant). In fact, during this process, the reaction takes place only at the interface, as a result, the high amount of oxidant is required for effective oxidation. Restrictions relating to the interphase mass transfer can be reduced in presence of heterogeneous catalysts [12]. Therefore, in the last years, the oxidation process has been carried over heterogeneous catalysts such as porous materials, due to their high surface area, which prepare a better interface for the organic and

aqueous phases. Among porous materials, ordered mesoporous silicas (with pore size > 2 nm) have received much attention due to their well-defined nano-size channels and large pore volume [13]. In 1992, Mobile company developed a new type of mesoporous silica M41S. These materials have high internal surface areas, uniform mesoporous aperture and easily controllable pore sizes. Because of these peculiar characteristics, the synthesis and application of mesoporous molecular sieves have been investigated by a large number of researchers [14]. MCM-41 is the most well-known member of M41S family, which contains a hexagonal array of one-dimensional channels of uniform mesoporous with a pore diameter of 2-10 nm with hydrophobicity and acidity property. Such special pore architecture makes it a suitable candidate for catalysis application [15]. Recently, there has been an increased interest in the insertion of metals with high redox potentials such as Ti into the original structure of the mesoporous silicas. This metal produces isomorphic substitutions that increase the catalytic activity in oxidative processes involving organic molecules of commercial products, such as phenols and bulky aromatics [16]. Although some researches propose microporous zeolite with the MFI morphology such as TS-1 (pore size < 2 nm) for ODS reactions, this kind of structures limit the accessibility of those compounds with the large molecular size (such as DBT and its derivatives) to the zeolitic pores. In contrast, the mesoporous silicas with the larger pore size have a better performance in oxidation reaction of big molecules [17, 18].

Lin *et al.* evaluated catalytic activity of Ti-MCM-41 nanoparticles in epoxidation of cyclohexene with aqueous H_2O_2, and they observed higher activity of the small particles compared with the micro sized particles in oxidation reaction [19]. Oxidative desulfurization of model sulfur-containing compounds with tert-butyl hydroperoxide in a continuous fixed-bed reactor has been investigated on Ti containing molecular sieves by Chica *et al.* and they found out that calcined Ti-MCM-41 particles revealed higher catalytic performance and slower deactivation rate compared with MoO_x/Al_2O_3 catalyst [17].

In the previous researches less studies have been focused on both synthesis and reaction conditions to achieve optimal conditions for ODS reaction of refractory sulfur compounds. In this work, Ti incorporated ordered mesoporous silicate particles, Ti-MCM-41, were synthesized by the hydrothermal method. As the porous structure and its property directly are dependent to the synthesis conditions [16], the impact of the composition of source materials such as TIPT (tetraisopropyl titanate)/TEOS (tetraethyl orthosilicate), NaOH (Sodium hydroxide)/TEOS, CTAB (cetyltrimethylammonium bromide)/TEOS molar ratio and also the crystallization temperature has been investigated on the structure of synthesized catalysts to achieve a catalyst with proper morphology, surface acidity, mesoporous structure and activity toward ODS reaction. In the ODS reaction of DBT with H_2O_2, based on the initial experiments that were done, the oxidant fraction and reaction temperature have been chosen as variable parameters because it was observed that although these parameters increase the reaction rate, they also produced water (from ODS reaction and thermal decomposition of H_2O_2) which hinders the rate of ODS reaction. Therefore, the effect of these opposing factors was investigated by a full factorial experimental design and the optimal conditions were obtained in the range of studied conditions on the base of the maximum DBT conversion. The reusability of Ti incorporated mesoporous silica was investigated for two times to study the ability of synthesized catalysts for further usage.

2. Experimental

2.1. Synthesis of catalysts

In-situ synthesis of Ti-MCM-41 was carried out by the hydrothermal method from tetra isopropyl titanate (TIPT 98 wt. %, Merck) as the titanium source, tetraethyl orthosilicate (TEOS 99 wt. %, Merck), as the silica source and cetyltrimethyl ammonium bromide (CTAB, Merck) as the organic template. Sodium hydroxide (NaOH > 97%) was used to create the basic media. All the chemicals were used with no further treatment. The synthesis procedure followed these stages: First, CTAB was dissolved in an appropriate amount of deionized water in a plastic container with a cap for 15 minutes with the magnetic stirrer at 500 rpm. After complete dissolution of CTAB to achieve better hydrolysis conditions for silica source to improve rate of the polymerization process, a proper amount of 2 M NaOH solution was added to the media. Then the mixture was stirred for 10 minutes. Thereafter, TEOS was added drop wise to the aforementioned solution during 20 minutes to be hydrolyzed. All the above steps were performed in ambient temperature and pressure. In order to have better dissolution of TIPT, the temperature of the mixture was raised to 313 K and kept for 10 minutes and then TIPT was added drop wise. After continuous stirring for 2 h at 500 rpm, the formed sol was transferred into a Teflon-lined stainless-steel autoclave for crystallization for 48 h. The crystallization temperature was changed in different conditions. The obtained white slurry was filtered, washed with DI

water, dried at 373 K overnight and finally calcined in air at 823 K for 6 h.

2.1.1. Operation conditions

There are many parameters affected on the morphology, structure and catalytic properties, including type and amount of surfactant, pH, calcination temperature, molar ratio of TIPT/TEOS, NaOH/TEOS, CTAB/TEOS, H_2O/TEOS, crystallization time and temperature. Based on primary experiments, the effective parameters such as crystallization temperature, TIPT/TEOS, NaOH/TEOS and CTAB/TEOS molar ratio were chosen as the operational variables to be studied. Other parameters such as water content, crystallization and calcination temperature were derived and fixed according to the literature. Table 1 shows the ranges of the considered variables such as; crystallization temperature (X_1: 323-383 K), TIPT/TEOS molar ratio (X_2:0.01-0.05), NaOH/TEOS molar ratio (X_3: 0.3-0.7) and CTAB/TEOS (X_4:0.1-0.2). The properties of the synthesized catalysts were analyzed based on characterization techniques.

2.1.2. Characterization of catalysts

The X-ray diffraction patterns of the samples were recorded with a STOE powder diffraction system in the 2θ range of 1-10° using Cu-Kα radiation (λ=0.154056). The morphology and particle size of the samples were obtained by Zeiss field emission scanning electron microscopy (FESEM) equipped with energy dispersive X-ray (EDX) analyzer. Functional group information of the samples was studied by Perkin Elmer Spectrum two fourier transform infrared (FTIR) measurements. The BET surface area and pore size distribution of the catalysts were measured by analysis of nitrogen isotherms collected at 77K using NOVA 2006 Quantchrome apparatus. The specific surface area and pore volume were determined from the N_2 adsorption-desorption at the relative pressure of $0.05<P/P_0<0.4$. Pore size distribution was calculated by Barrett-Joyner-Halenda (BJH) method from the adsorption branch of the N_2 physisorption isotherm.

2.2. Catalytic experiments

N-decane and dibenzothiophene were used as the model fuel and model sulfur compound, respectively. Acetonitrile was exploited as the polar solvent to extract DBT sulfones and sulfoxides from the organic phase. To prepare a solution as an appropriate model of real fuel, DBT with appropriate amount was dissolved in n-decane to obtain a solution with DBT weight content of 2300 ppm or 400 ppm sulfur.

Desulfurization of DBT was performed in a batch reactor fitted with magnetic stirrer and condenser at atmospheric pressure and moderate temperature as depicted in Fig. 1. When the water bath was adjusted at the required reaction temperature the feed (2300 ppm DBT in 25ml n-decane) was fed into the reactor, then an appropriate amount of H_2O_2 (35 wt. %) as oxidant and 0.5 gr catalyst were added and stirred with 500 rpm. After a period of time, the solution was treated by means of liquid-liquid extraction. In each extraction stage, an equal amount of acetonitrile was employed for all cases. The extraction at each step was performed as follows: equal volume of the fuel and acetonitrile were decanted into a glass beaker. The beaker was shaken for 5 minutes at room temperature. After separating the aqueous organic phases and acetonitrile, the final organic solution was analyzed by GC to detect the amount of DBT in the resultant model fuel.

Table 1. Ranges of the considered variables for synthesis of the catalysts.

Samples	Parameters			
	Crystallization temperature (K)	TIPT/TEOS (mol/mol)	NaOH/TEOS (mol/mol)	CTAB/TEOS (mol/mol)
S_5	323	0.01	0.3	0.1
S_7	383	0.01	0.3	0.2
S_8	323	0.05	0.3	0.2
S_6	383	0.05	0.3	0.1
S_3	323	0.01	0.7	0.2
S_1	383	0.01	0.7	0.1
S_4	323	0.05	0.7	0.1
S_2	383	0.05	0.7	0.2

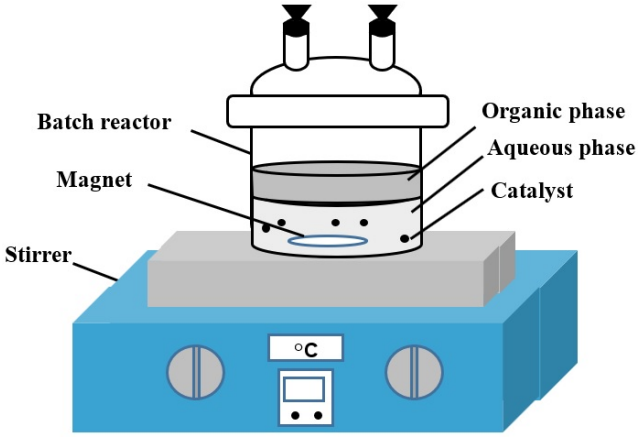

Fig. 1. Schematic of oxidative desulfurization unit.

At 10, 20, 30, 40, 60, 120, 180 and 220 min, respectively 1 µL of fuel sample was withdrawn and injected to the gas chromatography system (GC) coupled with a helium ionization detector (GC-HID) using a HP-5 capillary column, to detect sulfur containing compounds and identify their concentration in model fuel. In this analysis, helium was used as a carrier gas with the flow rate of 6 ml/min. First, the temperature of GC column was kept at 373 K for 2 minutes. Then it was heated from 373 to 553 K at 10 ˚C/min ramp rate with a final isothermal period of 10 minutes at 553 K.

Removal or conversion (X_a) of DBT was calculated using its initial concentration (C_0) and the concentration after a while (C_t) as follows:

$$\% \text{ DBT Conversion} = (C_0 - C_t)/C_0 \times 100$$

2.2.1. Experimental design

The removal efficiency of sulfur in oxidative process is affected by various parameters. Some of these parameters such as catalyst weight were fixed to reduce the number of experiments. The oxidant fraction and reaction temperature have been chosen as variable parameters. To evaluate the impact of the ratio of H_2O_2/DBT and reaction temperature on ODS efficiency; the experimental design with full factorial plan with one center point was employed. Experiments were performed in a random order to disperse the occurred random error in the whole region of experiments. These parameters and the resultant removal efficiency of sulfur are indicated in Table 2.

3. Results and Discussion

3.1. Mechanism of Synthesis

The proposed mechanism of Ti-MCM-41 formation is shown in Fig. 2 (4 steps). First, surfactant molecules in a certain concentration and pH are placed in a rod arrangement. After adding TEOS in basic media, hydrolysis of its molecules and creation of tetra-hydroxysilane molecules, due to the physical interaction between the positive charges of nitrogen groups at the end of the surfactant molecules with OH groups in tetra-hydroxysilane, its molecules are absorbed physically by the outer surface of the surfactant template. After allowing the basic solution, OH groups perform the condensation reaction with each other and Si-O-Si bridges are both formed around the micelles and in the length of the micellar rod. But since some of OH groups don't perform the condensation reaction, some of them remained freely inside or outside the cylindrical wall. Although this process was drawn only for one micellar surface, the same thing happens exactly during the micellar cylinders and silica walls are placed around the micellar cylinders [20, 21].

Table 2. Experimental design table for DBT conversion.

Experiments no.	Run order	Coded factors		Real factors		Responses
		X_1	X_2	Reaction temperature (K)	H_2O_2/DBT (mol/mol)	DBT removal (%)
1	Run1	-1	-1	313	5	62.8
2	Run2	+1	-1	343	5	78.6
3	Run3	-1	+1	313	20	67.1
4	Run4	+1	+1	343	20	83
5	Run5	-1	-1	313	5	62.2
6	Run6	+1	-1	343	5	80.1
7	Run7	-1	+1	313	20	65.2
8	Run8	+1	+1	343	20	83.5
9	Run9	0	0	328	12.5	84

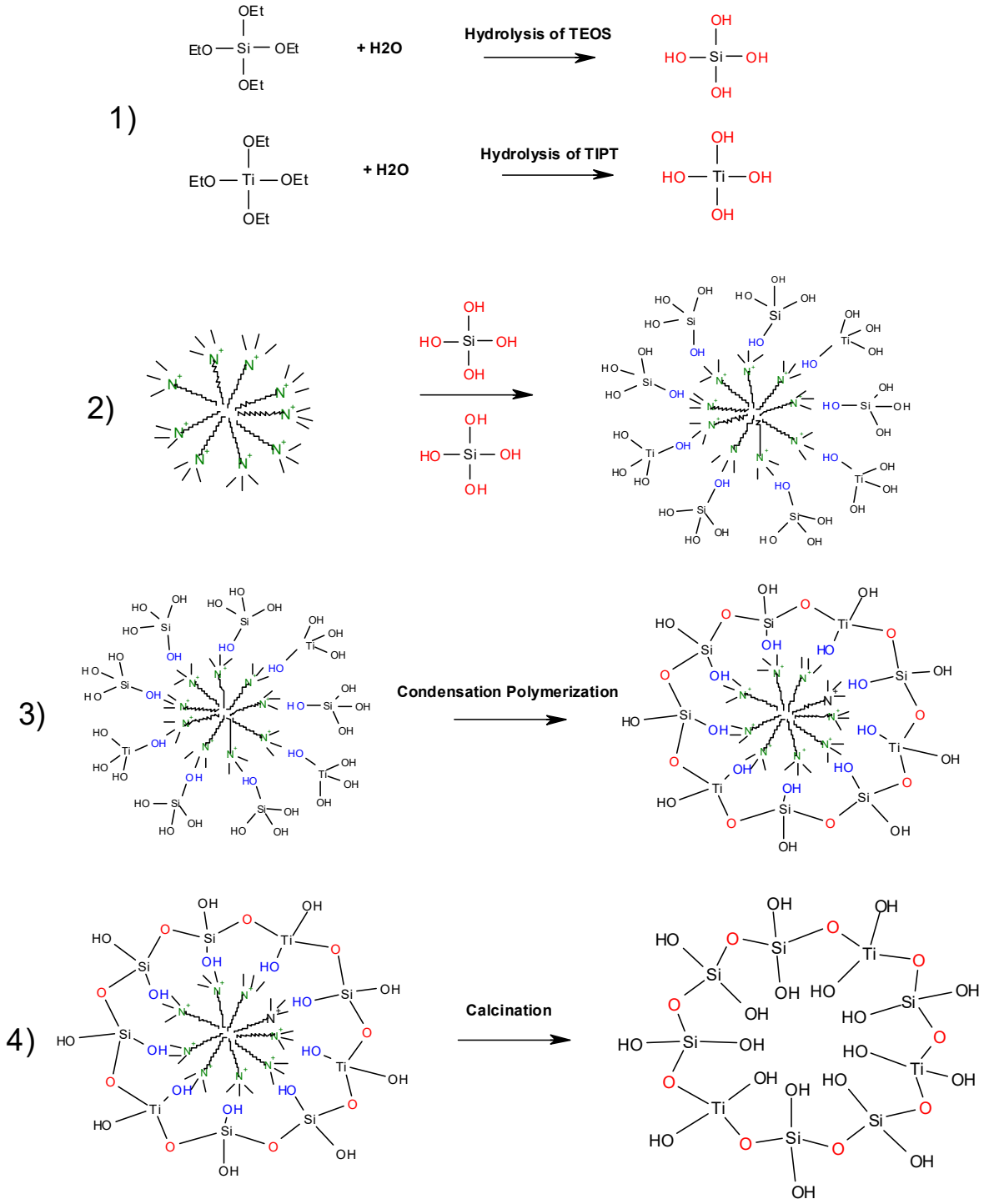

Fig. 2. Mechanism of Ti-MCM-41 Synthesis.

3.2. Characterization

3.2.1. X-ray diffraction

According to the X-ray diffraction pattern of mesoporous MCM-41 in the literature [22], this material has a peak with maximum intensity (100) in 2θ=21.2˚ and two weak peaks in 2θ=3.9 and 4.45˚ which can be indexed with (110) and (200) diffraction plane characteristics of well-ordered mesoporous structure. Although the Ti-MCM-41 structure has not been studied, researchers suggest that the presence of three peaks (100), (110) and (200) proving the hexagonal structure of MCM-41, with displacement of the peaks (due to the presence of Ti atoms) confirm formation of

Ti-MCM-41. Results of XRD analysis of Ti-MCM-41 samples are observed in Fig. 3(a) and 3(b). As can be seen in Fig. 3(a), those signals corresponding to (110) and (200) are poorly detected; therefore, the formation of Ti-MCM-41 crystals in S_1, S_2, S_3, S_4 and S_9 samples would not be confirmed, while in Fig. 3(b), all three mentioned index peaks can be recognized, so the crystal structure of Ti-MCM-41 related to S_5, S_6, S_7, S_8 and MCM-41 could be approved in accordance with the reference pattern.

It can be said that due to the high ratio of NaOH/TEOS in the synthesis gel of the S_1, S_2, S_3 and S_4 samples and presence of large fraction of OH^- ions, the hydrolysis rate of the silica source has been increased and the polymerization rate is decreased. In this case, the structure of material tends to form layer structures such as MCM-50 or other structures [23]. Given the higher rate of nucleation and crystal growth at high temperatures, it can be seen in Fig. 3a the intensity of index peak (100) related to S_1 and S_2 samples, which are synthesized at higher temperatures, is higher than the intensity of index peak related to S_3 and S_4 samples with the lower synthesis temperature. Also can be seen in Fig. 3(b), the intensity of index peak (100) relating to S_6, S_7 samples which are synthesized at higher temperatures, is higher than that in S_5 and S_8 samples with the lower synthesis temperature, which conforms to the literature [24].

Because of Ti present in MCM structure, the locations of 2θ relating to the peaks of (100), (110) and (200) would be shifted to the lower values and because of the higher radius of Ti_4^+ in comparison with Si_4^+, it indicates a larger distance between the layers. Increasing the distance between layers is related to the higher length of Ti-O bond compared with Si-O, therefore it revealed that entering Ti species causes slight expansion in the crystal structure against MCM-41 structure. This is why the value of 2θ relating to the peak of (100) in Ti-MCM-41 is lower than that impure MCM-41, as shown in Fig. 3(b).

Increasing CTAB/TEOS molar ratio leads to displacement in the location of index peaks to higher angular values [25] whereas increasing synthesis temperature acts in the opposite direction [24]. Although it seems there is interaction between these parameters, it can be seen from the XRD patterns (Fig. 3(a) and 3(b)) the effect of synthesis temperature is dominant. This is why the 2θ values relating to the peak (100), (110) and (200) in S_6 and S_7 samples, synthesized at 383 K, are less than the other samples of S_5 and S_8, synthesized at 323 K, in Fig. 3(b).

Also, it is shown in Fig. 3(b) that between pairs of (S_6 and S_7) and (S_5 and S_8) samples, S_7 and S_8, with the higher molar ratio of CTAB/TEOS, have higher 2θ values compared with S_6 and S_5 samples. Values of 2θ and d-space related to three index peaks for the reference sample (S_0) [23] and the other synthesized samples have been reported in Table 3. At the following sections, characterization analysis has been performed on the S_5, S_6, S_7 and S_8 samples which are confirmed on the base of their XRD patterns. MCM-41 would be studied as the base sample for comparison.

3.2.2. FE-SEM images and EDX

The FE-SEM images of the synthesized MCM-41 and Ti-MCM-41 samples are observed in Fig. 4. These images show the spherical and aggregate particles. The particle size of these samples is dependent on different parameters, however the synthesis temperature and the molar ratio of CTAB/TEOS are the most effective parameters. According to the literature [24, 25], increasing the synthesis temperature and the ratio of CTAB/TEOS, lead to an increase in the particle size of the samples.

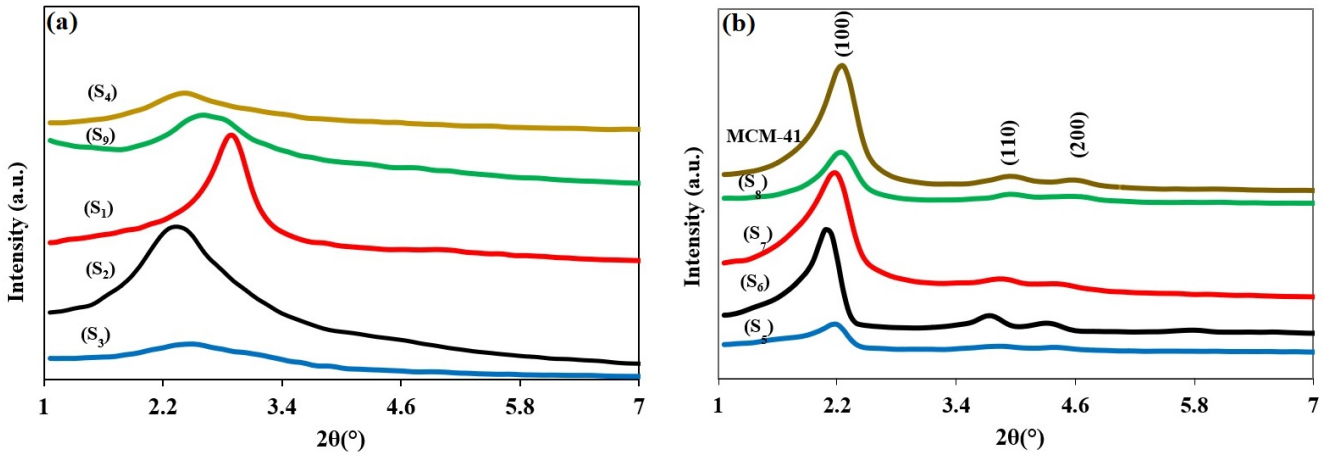

Fig. 3. XRD patterns of (a) S_1, S_2, S_3, S_4 and S_9, (b) S_5, S_6, S_7, S_8 and MCM-41samples.

Table 3. Results of XRD analysis and comparison with the reference peaks (S_0).

Samples	2θ			d-space (Å)		
	100	110	200	100	110	200
S_0	2.21	3.9	4.45	39.8	22.9	19.8
S_1	2.87	-	-	30.73	-	-
S_2	2.36	-	-	31.91	-	-
S_3	2.47	-	-	35.82	-	-
S_4	2.43	-	-	36.4	-	-
S_5	2.15	3.82	4.38	41.00	23.13	20.16
S_6	2.09	3.73	4.3	42.23	23.65	20.53
S_7	2.14	3.79	4.4	41.16	23.28	21.30
S_8	2.23	3.96	4.52	39.54	22.29	19.54
MCM-41	2.2	3.95	4.57	39.51	22.38	19.34

As can be seen from Fig. 4, the particle size of S_6, S_7 and MCM-41 samples synthesized at 383K are larger than the particle size of S_5 and S_8 samples synthesized at 323K. Between pairs of (S_6 and S_7) and (S_5 and S_8) samples, S_7 and S_8 synthesized with the higher ratio of CTAB/TEOS, have larger particles. In the S_5 sample, due to the low synthesis temperature and CTAB/TEOS molar ratio, the stage of crystal growth and separation of its core have not been well performed and according to the SEM image, it has shown agglomerated particles. EDX results of the elemental composition of S_5, S_6, S_7, S_8 and MCM-41 samples are shown in Fig. 5. As can be seen in this figure, the presence of Ti atoms in the structure of the samples has been confirmed and S_7 sample has the maximum ratio of Ti/Si.

3.2.3. FT-IR analysis

The FTIR spectrum of dried and calcined S_5, S_6, S_7, S_8 and MCM-41 samples in the range of 400-4000 cm^{-1} wavelength are depicted in Fig. 6. As shown in this figure, in all samples there is a broad peak at 3200-3400 cm^{-1} which is attributed to O-H vibrations of silanols. The peaks observed at 1250, 1085 and 462 cm^{-1} are related to bending vibration groups of Si-OH, asymmetric stretching vibration of Si-O-Si groups and bending vibration of Si-O-Si groups, respectively [16, 26]. The intensity of the mentioned peaks in S_6 and S_8 samples with less molar ratio of Ti/Si, is more than that of S_5, S_7 samples with the high molar ratio of Ti/Si. In the pure MCM-41, the intensity of aforesaid peaks is more than the other samples. The weak peaks at 910-960, 970 and 819-830 cm^{-1} are respectively related to stretching vibration groups Ti-O-Si, stretching vibration groups Si-OH and symmetric stretching vibration groups of Si-O. These bands are common characteristics of Ti-MCM-41 structure, which are the same as provided values in the literature [14, 27]. Considering the effects of synthesis temperature, precursors and the interaction of these parameters on the intensity of the bands, rigorous influences of each factor on FTIR patterns are difficult to be explained.

3.2.4. Reaction results and BET analysis

The catalytic ODS reaction and N_2 adsorption analyses were carried out on S_5, S_6, S_7, S_8 and MCM-41 samples to figure out the efficiency of each sample in sulfur removal and their specific surface area. The results can be seen in Table 4. It is concluded that S_5 and S_7 samples with higher surface area have revealed higher performance in ODS process and then MCM-41 has revealed the third order in catalytic activity. These three samples were selected for BET-BJH analysis to discuss their pore size and pore size distributions.

N_2 adsorption/desorption isotherms of S_5, S_7 and MCM-41 are presented in Fig. 7. These materials present the IV-type isotherm according to IUPAC classification that is related to mesoporous material with the pore size of 2-50 nm [26]. Isotherms of the samples show that in all three cases, the amount of adsorbed nitrogen has been increased by increasing relative pressure. At the relative pressure of about $P/P_0 \approx 0.3$ to 0.4, the amount of adsorbed nitrogen suddenly is increased to reach a roughly constant level. This phenomenon may be due to the uniform level of energy. The inset of Fig. 7 illustrates BJH pore size distribution curves of S_5, S_7 and MCM-41. The mesoporosity modal with narrow pore size distribution maximized at 2.9, 3.6 and 4.6 nm can be observed for S_5, S_7 and MCM-41, respectively.

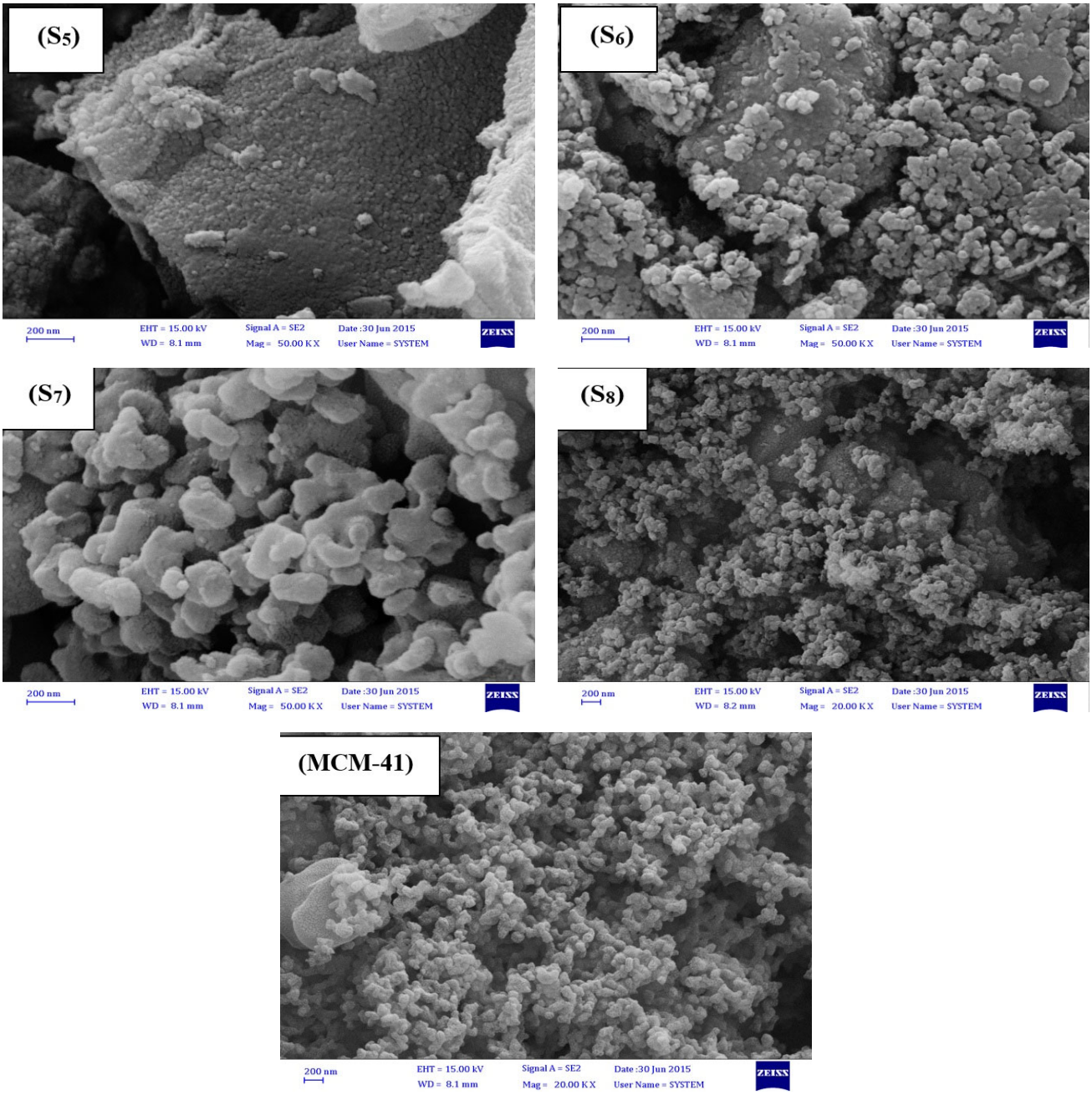

Fig. 4. SEM images of S_5, S_6, S_7, S_8 and MCM-41samples.

The pore size of the catalyst should be wide enough to allow diffusion of DBT molecules into the pores where most of the active sites are located, and also the DBT oxidation products which are bulkier compared to DBT with the molecular diameter of 1.7 nm could be able to leave the pores after reaction. Therefore, it can be said the reason for the lower efficiency of S_5 sample in the ODS process compared to S_7 (Table 4) may be due to its smaller pores. Also, in accordance with SEM results (Fig. 4) in S_5 sample due to the lower synthesis temperature, the stage of growth and separation of cores have not been accomplished and agglomerated particles are produced, as a result there is more resistance of mass transfer towards access of DBT molecules to the active sites. The less activity of MCM-41 rather than S_5 and S_7 would be related to the type of active sites which are not treated with titanium and it has caused the lower oxidation efficiency of DBT (as shown in Table 4). The results suggest that in addition to surface area the key factors affecting the activity of synthesized catalysts are pore size and Ti incorporation. In this study, finally S_7 sample with the suitable pore size and surface area and Ti/Si=0.01 was nominated to be investigated in further ODS reaction tests.

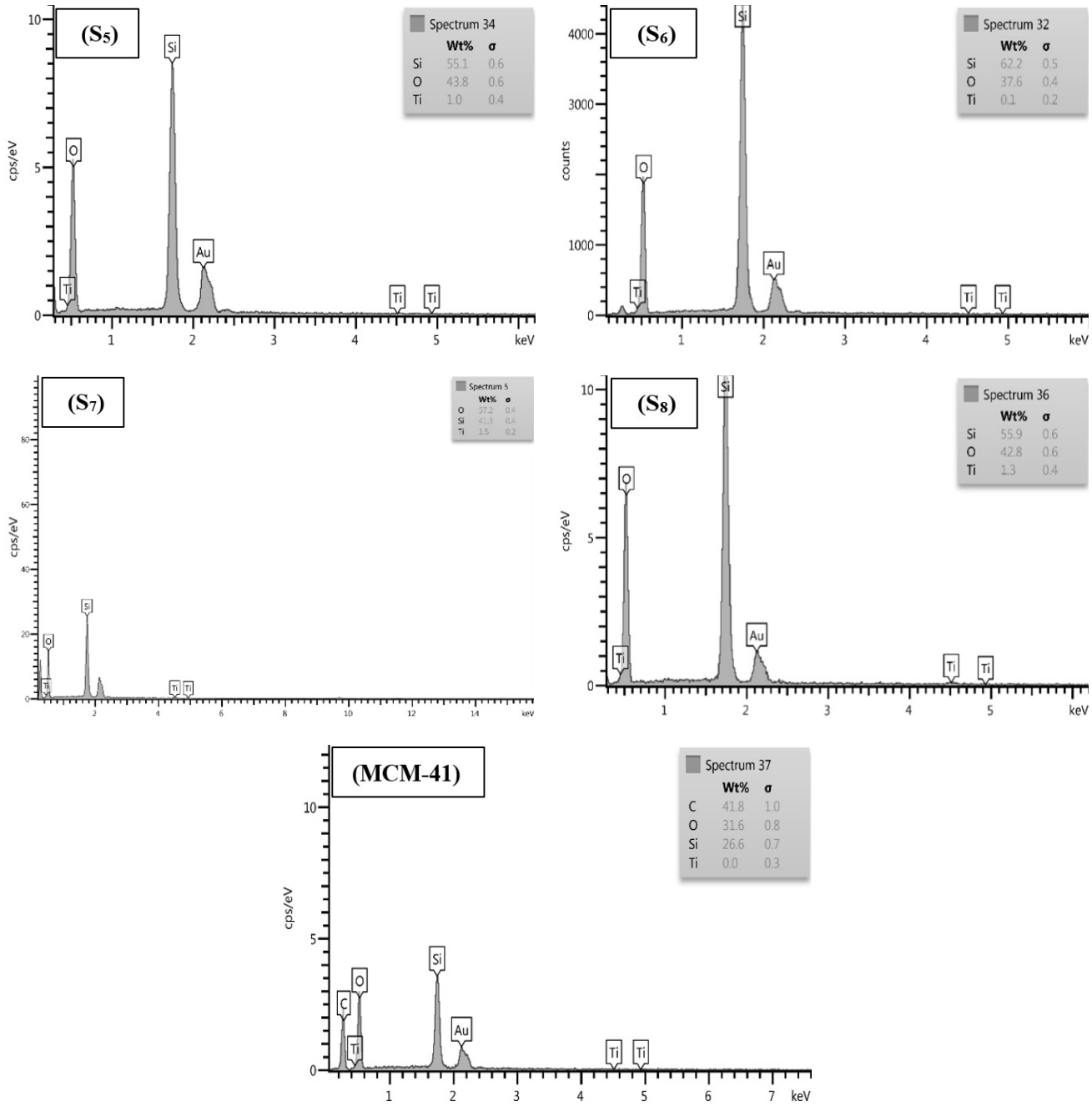

Fig. 5. Approximate elemental composition of the S_5, S_6, S_7, S_8 and MCM-41 samples by EDX.

3.3. Catalytic tests

3.3.1. Initial tests compared with blank

To evaluate the impact of oxidant and catalyst and the effect of Ti doped in MCM-41 on desulfurization process, five initial tests were conducted on the model fuel: (a) desulfurization over Ti-MCM-41 in the absence of H_2O_2, (b) desulfurization with H_2O_2 in the absence of catalyst, (c) extraction of DBT using acetonitrile in absence of catalyst and oxidant, (d) and (e) desulfurization over MCM-41 and Ti-MCM-41 in the same conditions (catalyst = 0.5 g, H_2O_2/DBT (molar ratio)= 12.5, T= 328 K), respectively. The results of DBT removal are presented in Fig. 8. The results of test (a) indicate that in the absence of oxidant, no reaction and not any DBT adsorption on catalyst would take place. The amount of DBT that is converted to the sulfones in test (b) is about 3% and test (c) indicates that about 35% of DBT can be extracted in the presence of acetonitrile.

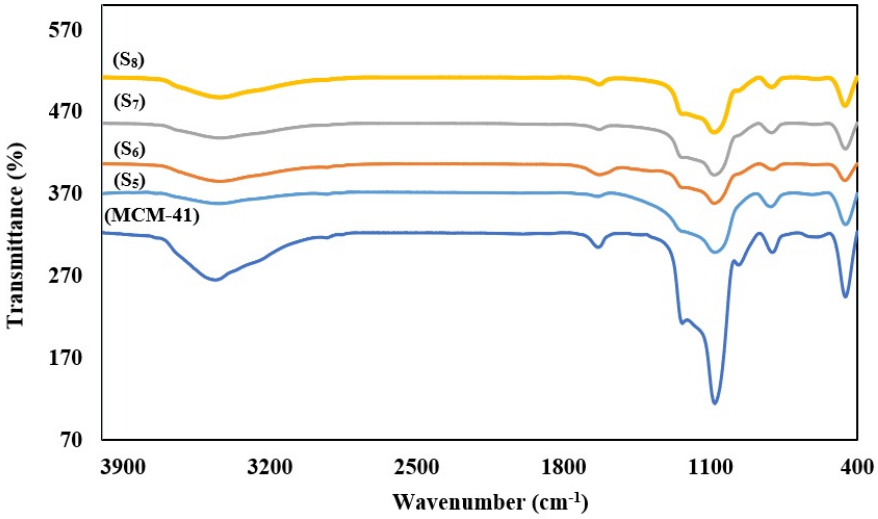

Fig. 6. FT-IR results of MCM-41, S_5, S_6, S_7 and S_8 samples.

Table 4. Single-point BET and conversion of ODS reaction.

Samples	Efficiency of desulfurization (%)[a]	Specific surface area (Single point) (m^2gr^{-1})
S_5	56.4	890
S_6	41	641
S_7	62	875
S_8	42.1	755
MCM-41	48.7	676

[a]Reaction condition: Feed= 1000 ppm DBT in 25ml n-decane, H_2O_2/DBT (molar ratio) = 5, T= 328 K.

Also, it can be seen in the results of tests (d) and (e), performance of S_7 in DBT removal from reaction is more than MCM-41 sample (about 7%). In fact, due to the coordinately unsaturated Ti cation species, catalytic activity of Ti-MCM-41 sample is improved in comparison with MCM-41 sample. DBT molecule can display Lewis basic character due to the available free ion electron pairs of this molecule. In result, DBT can be preferentially adsorbed by Ti-MCM-41 mesoporous surface according to a Lewis-type acid-base interaction. The adsorption of DBT on the catalyst surface can increase the collision probability of DBT and the catalyst active sites, which would accelerate the oxidation activity [27]. Test (f) indicate the use of homogeneous catalyst (formic acid) in the same conditions of desulfurization over MCM-41 and Ti-MCM-41, as it can be seen in this curve, with consumption of the high molar ratio of H_2O_2/DBT and Formic acid/DBT the efficiency of 55% is obtained.

3.3.2. Oxidesulfurization of DBT by Ti-MCM-41 (S_7 sample)

Results of oxidesulfurization experiments in different operating conditions according to the experimental design (Table. 2) in the presence of the best synthesized catalyst (S_7) are depicted in Fig. 9(a) and 9(b). Given that the reactive system consists of two liquid phases and a solid catalyst, the DBT removal would be calculated from DBT conversion in fuel phase analyzed by GC to evaluate removal of DBT. These experiments consist of two steps: The first step is oxidation of DBT and the second one is extraction of sulfones and unconverted DBT by acetonitrile. Fig. 9(a) presents the conversion of DBT versus time of reaction with one step extraction.

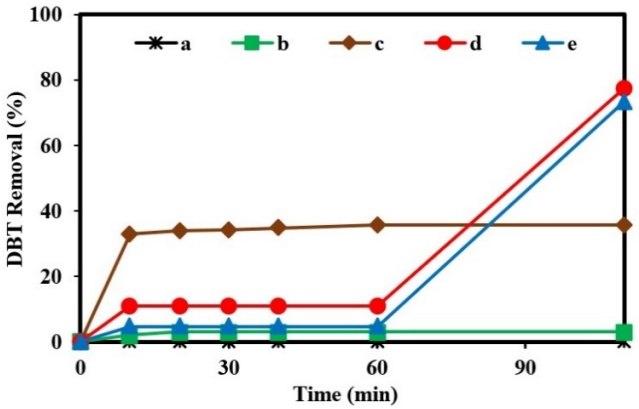

Fig. 7. N_2 adsorption-desorption isotherms and corresponding pore size analysis of S_7, S_5 and MCM-41.

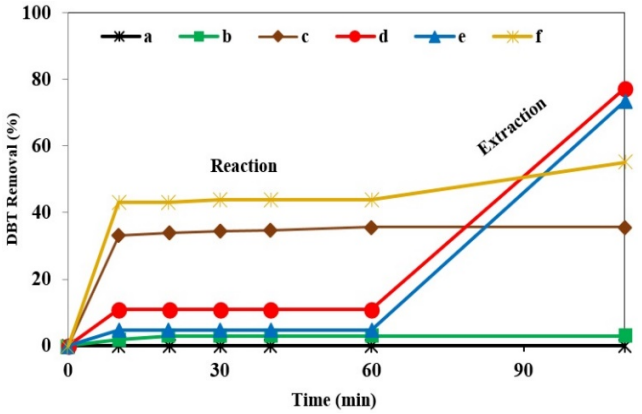

Fig. 8. Results of initial comparative blank tests in different conditions: a) Catalyst: 0.5 g of Ti-MCM-41, T= 328 K, in absence of oxidant. b) H_2O_2/DBT (molar ratio)= 15, T= 328 K, in the absence of catalyst. c) Acetonitrile/Feed (volume ratio)= 1, T= 328 K, in the absence of catalyst and oxidant. d) Catalyst: 0.5 g of Ti-MCM-41, H_2O_2/DBT (molar ratio)= 12.5 (solvent added after reaction), T= 328 K, e) Catalyst: 0.5 g of MCM-41, H_2O_2/DBT (molar ratio)= 12.5 (solvent added after reaction), T= 328 K, f) Formic acid/DBT= 22, Acetonitrile/Feed (volume ratio)= 1 (solvent added after reaction), H_2O_2/DBT (molar ratio)=27, T= 328 K.

Fig. 9(b) presents DBT removal before extraction (only by reaction) and by sequential reaction and extraction. As it can be seen the maximum removal DBT efficiency is obtained 84% that is related to Run4. It should be noted that the results are based on the average desulfurization efficiency obtained from two replicates.

To realize contribution of the catalyst in both adsorption and reaction process, the blank tests were conducted and it was realized that DBT would not be adsorbed on the catalyst surface (Fig. 8), whereas produced sulfones (here $DBTO_2$) would be adsorbed on the catalyst surface because of their polar property. The percentage of $DBTO_2$ that is adsorbed by the catalyst and also $DBTO_2$ that is left in the organic phase was calculated according to equations presented in Table 5 and the results are exhibited in Fig. 10 for five test runs.

3.4. Effect of operating conditions

As previously mentioned, the effect of parameters including H_2O_2/DBT molar ratio and the reaction temperature on DBT removal efficiency were studied, a full factorial design was implemented for the experiments. Fig. 11 represents a 3D plot of sulfur removal as a function of those two parameters. This figure also shows that at least one of these parameters has the effect of curvature. As can be seen in this figure, at the higher level of Oxidant/DBT (20), sulfur removal would be decreased gradually at the lower or higher temperatures. Also, when a high level of reaction temperature was applied (343K), the removal rate of sulfur was found to climb up and then decline by increasing Oxidant/DBT molar ratio.

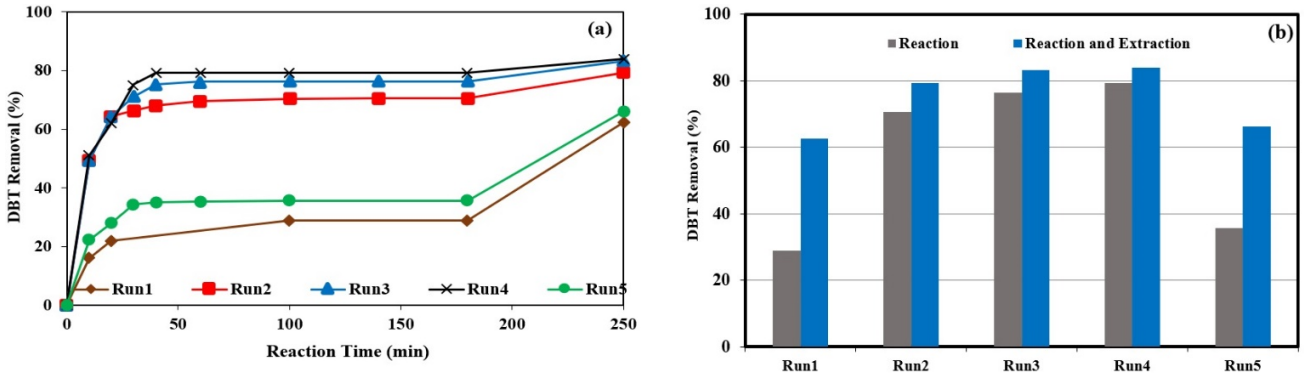

Fig. 9. Results of oxidesulfurization experiments in presence of S_7 catalyst: a) trends of DBT removal versus time with final step extraction by acetonitrile, b) the final percentage of DBT removal after reaction and after extraction.

Table 5. Base of calculations for DBT and its related sulfone (assumed $DBTO_2$) from reaction and adsorption in ODS processes.

No.	Relations
1	[a]DBT (Absorbed by the catalyst) = 0
2	DBT (Removed by reaction before extraction stage) = $DBTO_2$ (Total amount generated in the process)
3	$DBTO_2$ (Total amount generated) = $DBTO_2$ (Remained in organic phase) + $DBTO_2$ (Absorbed by Catalyst)
4	% $DBTO_2$ (Absorbed by Catalyst) = 1-[%$DBTO_2$ (Remained in the organic phase)]

[a]DBT is non- adsorptive component by the catalyst because of the blank test in Fig. 8 (part a).

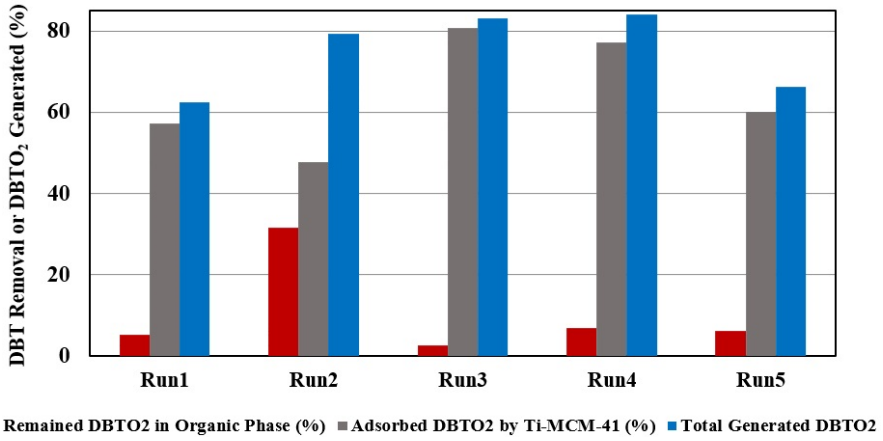

Fig. 10. Contribution of generated $DBTO_2$ in adsorption by the catalyst.

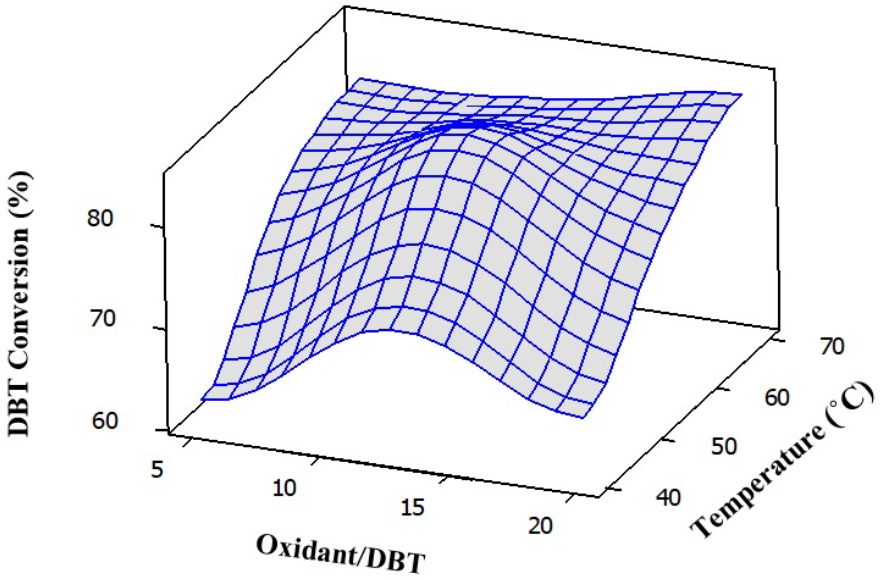

Fig. 11. Response surface plot for DBT conversion (Res.) as a function of temperature and H_2O_2/DBT.

These results show the importance of controlling these opposing factors. The excess amount of oxidant and reaction temperature would increase the ODS activity but the produced water (from ODS reaction and thermal decomposition of H_2O_2) hinders the rate of ODS reaction. The best result was obtained with the maximum DBT conversion of 84% using the 12.5 molar ratio of oxidant/DBT and reaction temperature of 328K.

3.5. Effect of acetonitrile solvent

At the further experiments, the extraction effect of acetonitrile in removal efficiency of sulfur compounds was investigated. Given that almost 35% DBT is extracted from the feed (resulted from blank tests), acetonitrile was added to the system at the beginning of ODS reaction. Therefore, part of available DBT was transferred from the organic phase to the aqueous phase and the rate of DBT removal was improved.

Fig. 12(a) displayed a comparison between the sulfur removal in Run2, Run3 and Run4 when acetonitrile was added after reaction and when it was added initially to the reaction system. As it can be seen in the second case, the higher amount of DBT has been removed from the fuel. As shown in Fig. 12(b), when acetonitrile was added initially to the system, the required time to achieve the maximum removal of DBT was reduced. It is resulted that Run 3 and Run 4 would achieve to their highest sulfur removal efficiency as higher than 99%.

Fig. 13 presents GC chromatograms of model oil in different stages of ODS for Run4 with maximum efficiency in removal of DBT. As it can be seen, DBT removal is achieved to 99.7% during 20 min using simultaneous reaction and extraction.

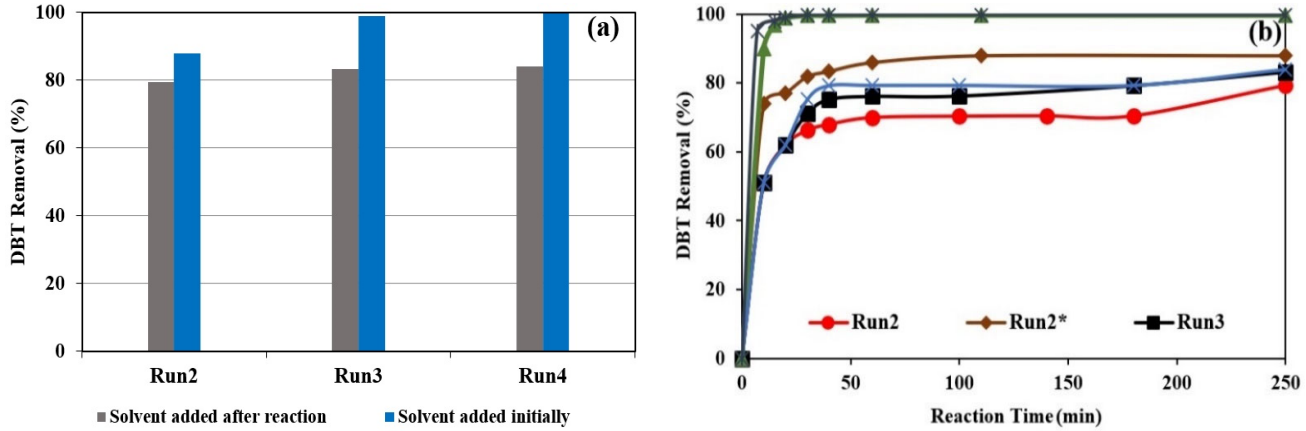

Fig. 12. a and b) DBT Removal from model fuel in various conditions (Run 2: T= 343 K and Oxidant/DBT molar ratio= 5, Run 3: T= 343 K and Oxidant/DBT molar ratio= 20, Run 4: T= 343 K and Oxidant/DBT molar ratio= 12.5.

3.6. Regeneration of catalyst

According to the appropriate performance of the sample S_7 in ODS process, the production of this sample is remarkable economically, due to employing low portion of template (CTAB), ease of synthesis and short crystallization time. For economical point of view, it is required to investigate stability of catalyst and its potential for regeneration. Therefore, catalyst recovery operations were performed by washing the catalyst samples with methanol and drying at 373 K for 4 hours. The recovered samples were implemented in ODS reaction at optimal operating conditions and the results are shown in Fig. 14. As it can be seen, after two reaction- regeneration cycles, approximately 6 and 11% of the catalyst performance have been reduced, respectively. It is expected that adsorption of highly polar DBT-sulfones on the surface of catalyst would be responsible for the catalyst deactivation.

3.7. Mechanism of oxidation

Oxidation of DBT actually contained two steps: first, DBT is oxidized into sulfoxide, which is the reaction determining step, and then further oxidization to the sulfones. In this study, the negligible amount of sulfoxides was detected by GC analysis under any reaction conditions. Therefore, the rate-determination step would be the oxidation of sulfide to sulfoxide, and sulfoxide formation is considered to dominate the reaction rate [28]. In fact, surface silanol groups of silica samples were performed as the catalytic active sites in oxidative desulfurization, while Ti atoms exist in the mesoporous structure improved the catalytic activity and selectivity [28, 29].

Fig. 15 illustrates the ODS reaction mechanism of DBT on the surface of titania-silica mesoporous catalyst, in presence of H_2O_2 as oxidant. As it can be seen, the first hydrogen peroxide is adsorbed on the surface of catalyst by coordination with Ti-OH and Si-OH surface groups. A five-member ring is formed via reciprocal hydrogen bonding, in which both the surface group and hydro peroxide serve as a hydrogen bond donor and acceptor. The electronic density of peroxy oxygen is lowered; therefore the electrophilicity of peroxy oxygen is prompted. When the sulfur atom of DBT nucleophilicly attacked the specific oxygen atom in the five-member ring (electrophilic oxidation), two protons are shifted and the transfer of the oxygen atom to DBT molecule would be occurred. DBT sulfoxide is formed and it is rate-determination step. The sulfoxide absorbs were formed on the active sites by a hydrogen bond with oxygen, the electronic density of sulfur atoms in sulfoxide is lowered, apparently activated for nucleophilic attack by the oxygen atom of unbound hydrogen peroxide. Hence, there is a reversal path in the mechanism from electrophilic oxidation to nucleophilic oxidation when sulfoxide is oxidized to sulfone in which this step reacts faster than the rate-determination step (sulfide to sulfoxide). Although the number of surface silanol groups are more than Ti-OH groups, the metallic property of Ti atom is more than Si atom. As a result, Ti atoms are more effective in electrophilic oxidation of DBT. The final sulfone product adsorption by Ti-OH and Si-OH surface groups on the active sites lead to hindrance of the next ODS reaction on the surface. Sulfones can be removed by methanol or ethanol after ODS reaction, for the regeneration of catalysts.

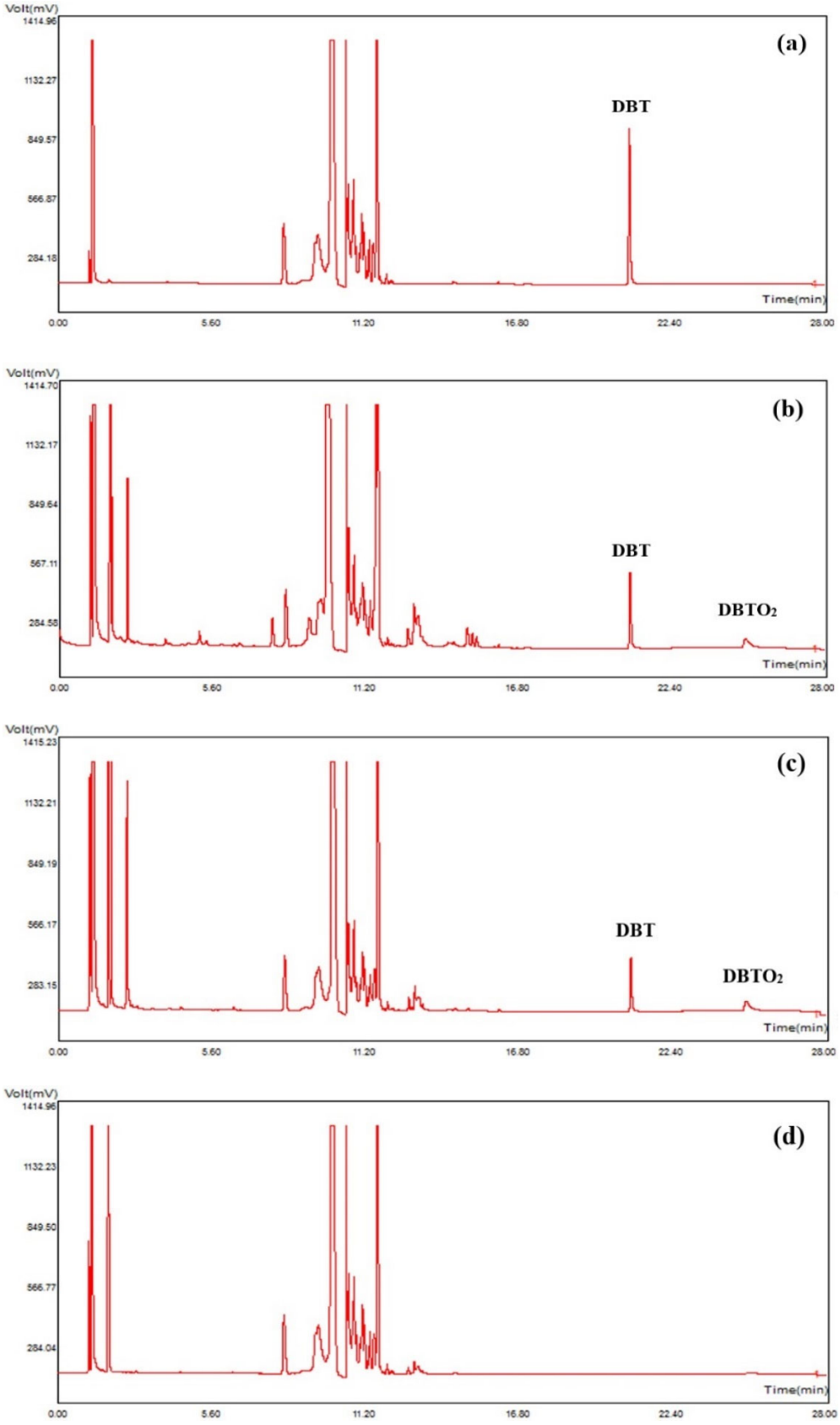

Fig. 13. GC chromatograms for the ODS of DBT in Run 4: a) feed containing 2300 ppm DBT, b, c, d) fuel phase after 5,10 and 20 min of starting process.

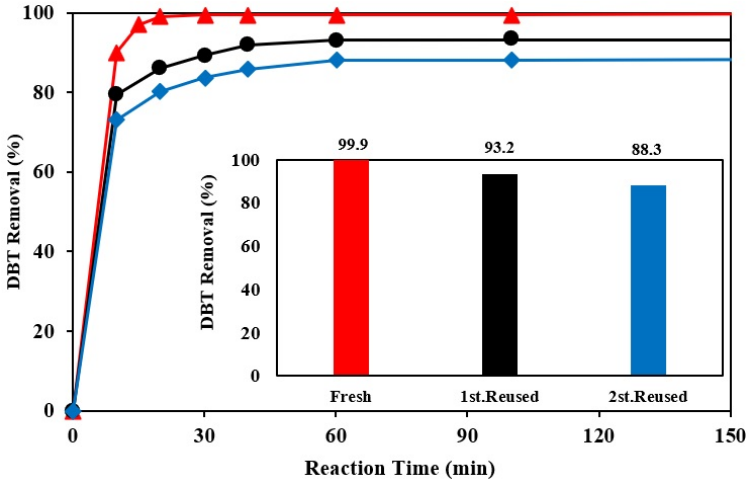

Fig. 14. Recovered catalyst performance in the removal of DBT from model fuel in the optimum conditions (when acetonitrile was added initially to the system), a) fresh, b) 1st reused, c) 2st reused.

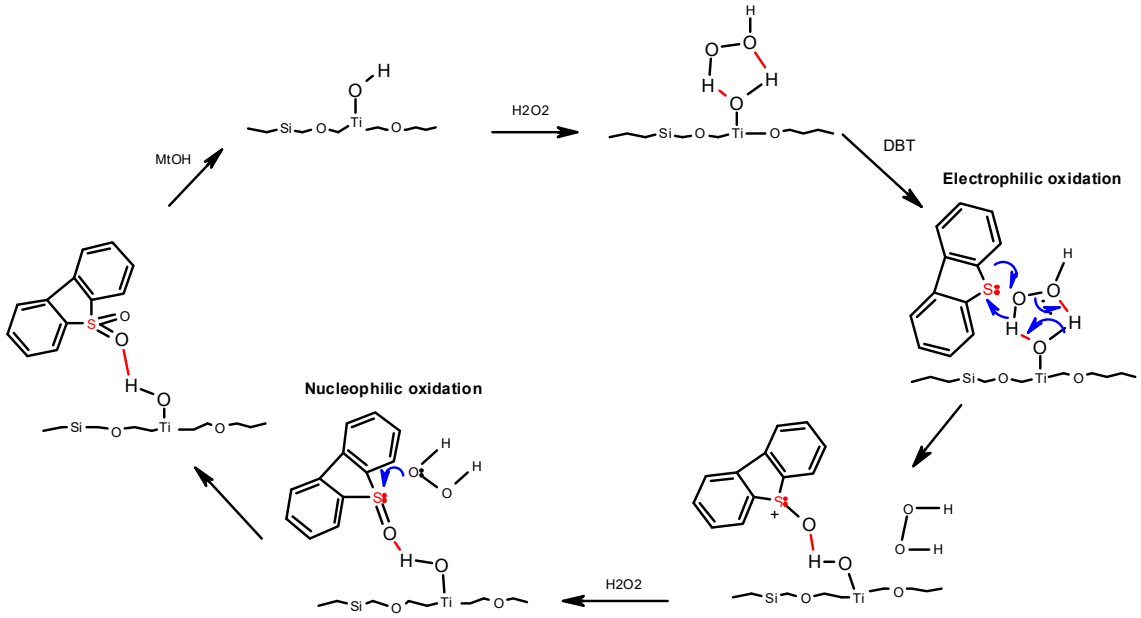

Fig. 15. The mechanism proposed for investigating the effect of surface-titania atoms on the DBT oxidation in the presence of hydrogen peroxide as an oxidizing agent (drawn with MDL ISIS/Draw software-version 2.5).

4. Conclusions

Different samples of Ti-MCM-41 as the mesoporous catalysts were synthesized by hydrothermal method to prepare the most efficient catalyst for ODS reaction. The molar ratio of NaOH/TEOS, CTAB/TEOS, TIPT/TEOS and synthesis temperature were the most influential parameters on the synthesis of highly ordered Ti-MCM-41 material. Reaction tests of DBT oxidation were carried out by hydrogen peroxide in the atmospheric pressure and different temperatures in the batch condition. Among different types of effective parameters, the reaction temperature and oxidant/DBT molar ratio were the most influential operating conditions. According to the results, the optimal operating conditions were determined at 328 K and the ratio of oxidant/DBT=12.5 to achieve 84% sulfur removal from the model fuel by the reaction. Also, it was concluded that Ti species in MCM framework improved the activity of the catalyst in ODS reaction. When acetonitrile was added initially to the reaction system the DBT removal was achieved up to 99.5% during 20 min reaction. The reusability of the catalyst was investigated and the recovered catalyst has shown about 11% decrease in catalytic performance. The adsorption of highly polar DBT-sulfones on the surface of the catalyst is responsible for the catalyst deactivation.

References

[1] A.E.S. Choi, S. Roces, N. Dugos, M.W. Wan, Sustainable Environ. Res. 26 (2016) 184–190.
[2] J. Chang, A. Wang, J. Liu, X. Li, Y. Hu, Catal. Today 149 (2010) 122–126.
[3] W. Ding, W. Zhu, J. Xiong, L. Yang, A. Wei, M. Zhang, H. Li, Chem. Eng. J. 266 (2015) 213–221.
[4] E. Kianpour, S. Azizian, Fuel 137 (2014) 36–40.
[5] H. Song, X. Wan, M. Dai, J. Zhang, F. Li, Fuel Process. Technol. 116 (2013) 52–62.
[6] G. Mohebali, A.S. Ball, Int. Biodeterior. Biodegrad. 110 (2016) 163–180.
[7] W. Liu, W. Jiang, W. Zhu, H. Li, T. Guo, H. Li, J. Mol. Catal. A: Chem. 424 (2016) 261–268.
[8] L. Cedeño-Caero, H. Gomez-Bernal, A. Fraustro-Cuevas, H.D. Guerra-Gomez, R. Cuevas-Garcia, Catal. Today 133-135 (2008) 244–254.
[9] J. Xiao, L. Wu, Y. Wu, B. Liu, L. Dai, Z. Li, H. Xi, Appl. Energy 113 (2014) 78–85.
[10] C. Ma, B. Dai, P. Liu, N. Zhou, A. Shi, L. Ban, H. Chen, J. Ind. Eng. Chem. 20 (2014) 2769–2774.
[11] L. Liu, Y. Zhang, W. Tan, Ultrason. Sonochem. 21 (2014) 970–974.
[12] T. Ren, J. Zhang, Y. Hu, H. Li, M.S. Liu, D.S. Zhao, Chin. Chem. Lett. 26 (2015) 1169–1173.
[13] R. Huirache-Acuña, R. Nava, C. Peza-Ledesma, J. Lara-Romero, G. Alonso-Núez, B.E. Pawelec, Materials 6 (2013) 4139–4167.
[14] A.E. Martinelli, J. Maria, D.F. Barros, U. Federal, Mater. Res. 18 (2015) 714–722.
[15] P.S. Sathish Kumar, M. Ruby Raj, S. Anandan, Sol. Energy Mater. Sol. Cells 94 (2010) 1783–1789.
[16] R.S. Araújo, F.S. Costa, D.A.S. Maia, H.B. Sant Ana, C.L. Cavalcante, Braz. J. Chem. Eng. 24 (2007) 135–141.
[17] A. Chica, A. Corma, M.E. Dómine, J. Catal. 242 (2006) 299–308.
[18] K. Lin, P.P. Pescarmona, H. Vandepitte, D. Liang, G. Van Tendeloo, P.A. Jacobs, J. Catal. 254 (2008) 64–70.
[19] K. Lin, P.P. Pescarmona, K. Houthoofd, D. Liang, G. Van Tendeloo, P.A. Jacobs, J. Catal. 263 (2009) 75–82.
[20] C.Y. Chen, S.L. Burkett, H.X. Li, M.E. Davis, Microporous Mesoporous Mater. 2 (1993) 27–34
[21] M. Nekoomanesh, H. Arabi, G.R. Nejabat, M. Emami, G. Zohuri, Iran. J. Polym. Sci. Technol. 21 (2008) 243-250.
[22] H. Wang, P. Van Der Voort, H. Qu, S. Liu, J. Nanopart. Res. 15 (2013) 1501-1504.
[23] J.S. Beck, J.C. Vartuli, W.J. Roth, M.E. Leonowicz, C.T. Kresge, K.D. Schmitt, J.L. Schlenkert, J. Am. Chem. Soc. 114 (1992) 10834–10843.
[24] Y. Chen, X. Shi, B. Han, H. Qin, Z. Li, Y. Lu, Y. Kong, J. Nanosci. Nanotechnol. 12 (2012) 7239–7249.
[25] H.I. Meléndez-Ortiz, L.A. García-Cerda, Y. Olivares-Maldonado, G. Castruita, J.A. Mercado-Silva, Y.A. Perera-Mercado, Ceram. Int. 38 (2012) 6353–6358.
[26] N.N. Opembe, E. Vunain, A.K. Mishra, K. Jalama, R. Meijboom, J. Therm. Anal. Calorim. 117 (2014) 701–710.
[27] X.M. Yan, P. Mei, J. Lei, Y. Mi, L. Xiong, L. Guo, J. Mol. Catal. A: Chem. 304 (2009) 52–57.
[28] D. Wang, N. Liu, J. Zhang, X. Zhao, W. Zhang, M. Zhang, J. Mol. Catal. A: Chem. 393 (2014) 47–55.
[29] D. Marino, N.G. Gallegos, J.F. Bengoa, A.M. Alvarez, M.V. Cagnoli, S.G. Casuscelli, S.G. Marchetti, Catal. Today 133 (2008) 632–638.